applied optics

Modified surface testing method for large convex aspheric surfaces based on diffraction optics

Haidong Zhang,[1,2] Xiaokun Wang,[1,*] Donglin Xue,[1] and Xuejun Zhang[1]

[1]Changchun Institute of Optics, Fine Mechanics and Physics, Chinese Academy of Science, Changchun 130033, China
[2]University of Chinese Academy of Sciences, Beijing 100049, China
*Corresponding author: jimwxk@sohu.com

Received 18 August 2017; revised 30 October 2017; accepted 30 October 2017; posted 30 October 2017 (Doc. ID 305164); published 22 November 2017

Large convex aspheric optical elements have been widely applied in advanced optical systems, which have presented a challenging metrology problem. Conventional testing methods cannot satisfy the demand gradually with the change of definition of "large." A modified method is proposed in this paper, which utilizes a relatively small computer-generated hologram and an illumination lens with certain feasibility to measure the large convex aspherics. Two example systems are designed to demonstrate the applicability, and also, the sensitivity of this configuration is analyzed, which proves the accuracy of the configuration can be better than 6 nm with careful alignment and calibration of the illumination lens in advance. Design examples and analysis show that this configuration is applicable to measure the large convex aspheric surfaces.

OCIS codes: (120.3940) Metrology; (220.1250) Aspherics; (090.1000) Aberration compensation; (050.1970) Diffractive optics.

https://doi.org/10.1364/AO.56.009398

1. INTRODUCTION

Aspheric surfaces are widely used in the modern optical systems for their excellent properties, such as reducing aberrations, decreasing the number of optical elements, lightening the optical system, increasing the transmittance of the system, and so on [1]. With the demand of aspheric surfaces increasing, highly accurate surface testing has been a challenge, especially for large convex aspheric surfaces. It is because concave aspheric surfaces can be interferometrically measured from the center of curvature with a null corrector, while it is difficult to collect the testing rays reflected from the convex aspheric surface under test.

The method based on an aberration-free point uses the Hindle sphere to collect and bring the rays, reflected from the convex surface under test, back via the same path [2–4]. The shortcoming of this method is that: (a) the auxiliary mirror is commonly several times the aperture of the surface under test, which is difficult to be manufactured with high accuracy when the convex asphere under test is too large. (b) It can measure only the conic surfaces, except the convex ellipsoid surface, and also it has an obstructed aperture.

The null lens and computer-generated hologram (CGH) are commonly used to correct the aberrations of test lights [5–7], which need to be specially designed for each aspheric surface. The null lens is often made up of two lenses, and the last surface is aspheric generally [8,9], which leads to the high manufacturing cost. The CGH has been an important tool to measure aspheric optics, but the bottleneck of CGH is that the manufacturing precision decreases as the aperture of CGH increases. The CGH usually is fabricated no more than 200 mm with high accuracy. Even though the CGH can be used with the subaperture stitching method to expand the testing area [10,11], due to this dimensional limitation, the efficiency and accuracy of the subaperture stitching method will suffer a lot.

The method proposed by Burge uses a CGH based on a Fizeau interferometer to make subaperture measurements on large convex aspheric surfaces [12–14]. It is quite innovative because the hologram pattern is written directly on the concave surface of the test plate, so all of the surfaces used in the configuration are spherical. But only concentric rings can be written directly onto the concave spherical surface with high precision [15], which means the non-rotational symmetric surfaces cannot be measured with high accuracy.

In this paper, we propose a modified method that utilizes a relatively small CGH and an illumination lens to measure large convex aspheric surfaces. It also can be combined with the subaperture stitching test method to expand the whole measuring area. This will substantially improve the efficiency and accuracy, since it enlarges the area of single testing. This layout tactfully avoids the overly dimensional demand on CGH, and the illumination lens also has a certain feasibility. For those who measure large aspheric surfaces, the method proposed in this paper can make them get rid of large auxiliary mirrors, which are commonly several times the aperture of the surface under test. And also, it will bring about higher measurement

efficiency benefiting from fewer subapertures and lower cost arising from fewer null correctors. In Section 2, the principle of this method and some key optical elements in this configuration are described in detail. In Section 3, the limitation of this arrangement and the range of application for mirrors with different parameters are discussed. We also discuss the feasibility of the illumination lens that one lens can be used to measure a range of aspheric surfaces with different parameters. In Section 4, two design examples are given to demonstrate the feasibility and applicability of this method, and proper tilt carrier frequency is also employed into the CGH to split spurious diffraction orders. After this, the sensitivities of this arrangement, including adjusting errors and manufacturing errors, are analyzed in Section 5.

2. PROPOSED METHOD

A. Principle of This Method

The schematic layout is shown in Fig. 1. The light beam, emerging from the interferometer, incidents the transmission sphere and turns into the spherical wavefront, and then, the spherical wavefront goes through the CGH and illumination lens successively. The purpose of the illumination lens is turning a diverging wavefront into a converging one, and we take advantage of a specific CGH to make the first-order diffraction light incident the surface under test perpendicularly. The reflected light, bringing the information of the aspheric surface, interferes with the reference light produced from the transmission sphere. We then get the surface figure error by analyzing the interferograms. The CGH is placed outside the focus of the interferometer because all spurious diffraction orders can be separated by employing proper tilt carrier frequency into the CGH and blocked by the filter located at the focus of the interferometer, while when the CGH is placed inside the focus, all spurious diffraction orders during the second passage of CGH can be blocked only by the inner filter of the commercial interferometer. The diameter of the pinhole on the filter is about 2 mm.

B. Some Optical Elements in the System

1. Interferometer and Transmission Sphere

The interferometer is widely applied in surface testing, which has a high accuracy. The interferometer in this system is a general commercial Fizeau interferometer, which is very easily available in optical shops. The transmission sphere is used to get a spot light and produce the reference wavefront, which is reflected from the last surface of the transmission sphere. There is a rule for the choice of the transmission sphere:

$$F/\# \le R/\#. \tag{1}$$

$F/\# = F/D$, where F is the focal length of the transmission sphere, and D is the diameter of the transmission sphere; and $R/\# = r/d$, where r is the distance between the focus of the interferometer and CGH, and d is the diameter of CGH.

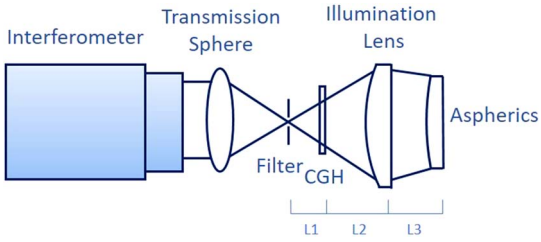

Fig. 1. Schematic layout for the test arrangement. The CGH is located outside the focus of the interferometer. All disturbing orders are blocked by the filter placed at the focus and the filter inside the commercial interferometer. L1 is the distance between the focus of the interferometer and the CGH; L2 is the distance between the CGH and the illumination lens; and L3 is the distance between the illumination lens and the aspheric surface to be tested.

2. Computer-Generated Holograms

The CGH is designed specifically to correct the aberrations of a convex aspheric surface and illumination lens. Therefore, the first-order diffraction light is the aspheric wavefront that is fitted to the convex surface under test. We use 37-term Zernike polynomials to describe the phase of CGH in Zemax software. Considering this measuring system is not a common path arrangement, we here apply the amplitude-type CGH to compensate the errors introduced in the testing path, because the manufacturing precision of amplitude-type CGH is higher than phase-type CGH. We should also take fringe contrast into consideration, and the contrast of fringe is as follows:

$$\begin{aligned} I_r &= 4\% \\ I_t &= 96\% \times 10\% \times 96\% \times 96\% \times 40\% \\ &\quad \times 96\% \times 96\% \times 10\% \times 96\% \\ &= 0.31\% \\ I_{\max} &= I_r + I_t + 2\sqrt{I_r I_t} = 0.04 + 0.0031 + 0.022 = 0.0651 \\ I_{\min} &= I_r + I_t - 2\sqrt{I_r I_t} = 0.04 + 0.0031 - 0.022 = 0.0211 \\ V &= \frac{I_{\max} - I_{\min}}{I_{\max} + I_{\min}} = 0.51, \end{aligned} \tag{2}$$

where I_r is the reference light intensity, I_t is the test light intensity, $I_{\max}$ is the maximum intensity of interference fringe, $I_{\min}$ is the minimum intensity of interference fringe, and V is the fringe visibility.

The first-order diffraction efficiency of amplitude-type CGH is about 10%, the transmittance of glass is 96%, and the reflectivity of SiC is 40%. The fringe visibility of 0.51 is acceptable.

The CGH has several areas: one main functional area for correcting aberrations of the testing wavefront; two alignment areas for adjusting relative position, including piston, tilt, and decentration between the CGH and interferometer, and between illumination lens and CGH; and also some fiducial areas for imaging crosslines to the illumination lens and convex aspheric surface to determine the lateral position. The layout is shown in Fig. 2. The auxiliary areas can make the alignment more accurate.

3. Illumination Lens

The difficulty of testing a large convex surface is that it is hard to collect the rays reflected from the convex surface. The illumination lens here solves the problem in this configuration. The lens is located close to the convex surface to be tested, and the gap between these two optical elements is less than 50 mm, thus the aperture of the illumination lens needs to be just slightly larger than the convex aspheric surface in full aperture

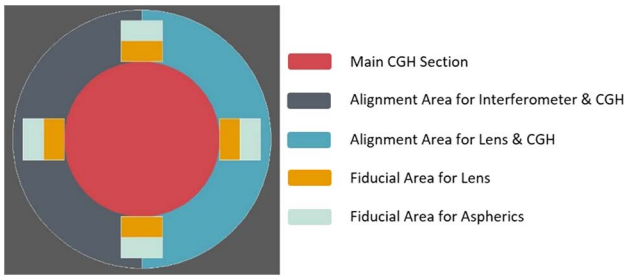

Fig. 2. Layout of CGH. The middle red area is the main functional area for correcting the aberrations of test lights. The gray and cyan zones are two alignment areas, and others are the fiducial areas for adjusting the CGH, illumination lens, and convex surface under test.

measurement. The lens here is a plano-convex lens, since it can be more easily and accurately manufactured than a biconvex lens. It should be noted that the convex surface of the illumination lens is toward the CGH. It is because any tilt, decentration, or lateral translation of the illumination lens can be reflected by the interference fringe of the alignment area in this situation, while only tilt can be observed if the plane is toward the CGH. It benefits the adjustment of the illumination lens on high precision.

The illumination lens plays an important role in the configuration and has effects on the accuracy of the setup. The illumination lens can be manufactured by continuous polishing technology and further polished by the ion beam figuring (IBF) technology. The radius of curvature and surface figure error of the illumination lens can be tested by a coordinate measuring machine (CMM) and subaperture stitching interferometer (SSI), respectively. With a couple of iterations, the illumination can be fabricated within $1/100\lambda$ RMS.

The diameter of the illumination lens is generally between 300 mm and 500 mm. Therefore, the area of single measurement is no more than 500 mm. But we can use the subaperture stitching method to expand the whole measuring area.

3. DISCUSSION

A. Application Range of This Configuration

In this arrangement, it has dimensional limits for both CGH and the illumination lens. For CGH, it is composed of a range of wavy lines that can be fabricated with high precision within 200 mm diameter by a laser direct writing system. When the diameter of CGH is more than 200 mm, the processing accuracy will be affected. For the illumination lens, a larger lens means a larger test region in this arrangement, which is significantly important in the subaperture testing method, as it can reduce the number of measurements to be needed to cover the full aperture. However, the large lens improves processing difficulty and production cost. We thus design the illumination lens no more than 500 mm under the trade-off among these aspects. Because of the restriction of the factors above, this method has a certain application range.

When the $R/\#$ of a convex aspheric surface is small or the conic constant K of aspherics is large, it needs a steeper illumination lens to converge the light. That will introduce more spherical aberration in this system and enlarge the caustic region. What should be noted is that the CGH must be located far away from the caustic area, because light beams in the caustic region interweave together, and one point of CGH cannot correct aberrations for two directions. When the caustic region enlarges, the size of CGH is forced to be larger.

For acquiring the relationship between the size of CGHs and the parameters K and $R/\#$ of the aspheric surfaces, a variety of experiments are operated. To avoid introducing large aberrations by a steep illumination lens, the distance between illumination lens and the focus of the interferometer should not be too short. It is assumed that this distance ranges from 7000 mm to 8000 mm by changing the radius of the convex surface of the lens, and the gap between the illumination lens and aspheric surface is fixed at 40 mm. For aspheric surfaces ($D = 500$, 400, and 300 mm and $K = 0$ and -5), various CGHs are designed with the residual aberrations of wavefront no more than 0.002λ (RMS) ($\lambda = 632.8$ nm). The minimum size of CGH to be needed L versus the $R/\#$ of the surface under test for different apertures and conic constant K is shown in Fig. 3. Based on that, the limitation of the diameter of CGH (main section area) is 200 mm, and all aspherics with $D \leq 500$ mm and $K \leq -5$ can be measured when the $R/\#$ is larger than $R/6.2$. When the diameter of aspherics is 300 mm, the minimum $R/\#$ that can be tested is $R/4$. For the same $R/\#$, a larger test area needs larger CGH, so the distance between the convex asphere under test and the illumination lens should not be too long.

B. Universality of the Illumination Lens

In the null testing method, the phase correctors usually need to be specially designed according to each aspheric surface, and this will raise testing cost inevitably. The CGH in this configuration is also specific; however, the illumination lens has certain universality. One illumination lens can cover a variety of aspheric surfaces with different parameters. Assuming that the diameter of the testing area is 400 mm, a series of aspheric surfaces, with parameters $R/\#$ from $R/6$ to $R/10$ and the conic constant K from -1 to -5, can be tested with two illumination lenses and specific CGHs according to our designed experiments. All the sizes of the main CGH sections are less than 200 mm, and the residual of aberrations are less than 0.001λ (RMS) (Fig. 4).

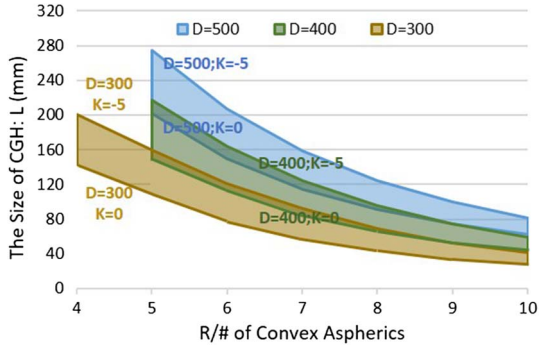

Fig. 3. Minimum size of CGH to be needed L versus the $R/\#$ of surfaces under test for different apertures and conic constant K. The value of the L decreases as the $R/\#$ increases, or the aperture and conic constant K decrease.

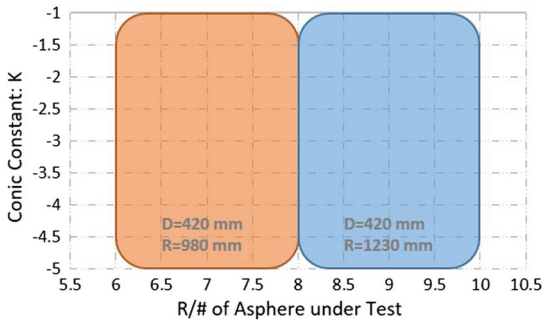

Fig. 4. Two plano-convex illumination lenses cover a variety of aspheric surfaces with different parameters. The left lens with $D = 420$ mm, $R = 980$ mm corresponds to aspheric surfaces with K from −1 to −5 and $R/\#$ from $R/6$ to $R/8$, while the right one can measure aspheric surfaces with K from −1 to −5 and $R/\#$ from $R/8$ to $R/10$.

The illumination lens with $D = 420$ mm and $R = 980$ mm can be used with specific CGHs together to measure the convex aspheric surfaces when the parameter K is from −1 to −5 and $R/\#$ is from $F/6$ to $F/8$, while the other one with $D = 420$ mm and $R = 1230$ mm can be utilized to measure convex aspheric surfaces when the parameter K is from −1 to −5 and $R/\#$ is from $F/8$ to $F/10$. From our experiments, we know that the illumination lens has certain universality. With appropriate planning of parameters, it can reduce testing cost and consume less time by illumination lenses.

4. DESIGN EXAMPLES

To demonstrate the feasibility and applicability of this method, two systems are designed for this method. One is 320.8 mm diameter convex aspherics ($R/12.76$) measured by this method and the other is 800 mm diameter convex asphrics ($R/3.75$) tested by the combination of this method and the subaperture stitching method.

A. Full-Aperture Test on the Large Convex Aspheric Surface

The convex aspheric surface in this case is a hyperbolical mirror, and its structure parameters are shown in Table 1. In the Hindle sphere method, the auxiliary mirror is at least 500 mm, and in the conventional CGH method, it needs 2 CGHs to measure the whole area. In our configuration, it needs only one CGH and an illumination lens with $D = 326$ to test this aspherics.

The asphere departure and asphere departure slope of this convex surface are shown in Fig. 5. It indicates that this convex mirror is a weak asphere.

We first complete the design of the illumination lens mainly considering the practical focus. A long light path will bring

Table 1. Structure Parameters of the Aspheric Surface

Vertex Curvature of Radius/mm	Aspheric Coefficient	Diameter/mm	Material
4093.72	−3.662	320.8	SiC

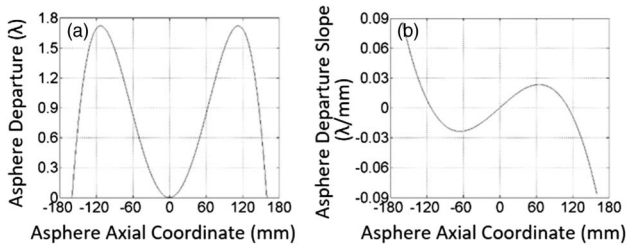

Fig. 5. (a) Asphere departure of this asphere. The max value is no more than 1.8λ. (b) Asphere departure slope of the convex aspheric surface. The max slope is less than 0.1λ/mm.

trouble to the alignment while too short a distance will introduce more aberrations. After that, the CGH can be designed by using 37 Zernike polynomials in Zemax software. The parasitic diffraction orders can be separated by employing appropriate tilt carrier frequency and a filter located at the focal plane. The parameters of this system and optical elements are shown in Table 2.

The system is designed with Zemax, shown in Fig. 6(a). We take advantage of a 326 mm illumination lens and a 94.4 mm CGH (main section area) to test the convex asphere with $D = 320.8$ mm. The minimum line spacing of the CGH is 18 μm, which can be fabricated at high precision. Because of the tilt carrier frequency employed in the CGH, the focus of the CGH is off axis. The lateral departure of the CGH is 16.186 mm. The parasitic diffraction orders can be separated by a filter with a 2 mm diameter pinhole, and the separated disturbing diffraction orders in the filter plane are shown in Fig. 6(b).

The light beam produced from the interferometer passes through the CGH twice and derives many diffraction orders. The multiple diffraction orders are represented by (m, n), where m is the order that the light beam passes through the CGH for the first time, and n is the order during the second time. We here focus on the diffraction orders (1, 0) (1, 2) (0, 2) (2, 0) (−1, 3), and (3, −1). It is because the orders (m, n), with $m + n - 2 = 0$, $(m - 1)(n - 1) = 0$ and $(m + n - 2)(m - 1)(n - 1) \neq 0$, are stubborn orders that are close to the order

Table 2. Parameters of the System and Designed Optics for the Convex Conic Surface with $D = 320.8$ mm ($R/12.76$)

Parameters of the CGH		Value (mm)	Parameters of System	Value (mm)
Lateral departure		16.186	Distance L1	1200
CGH thickness		10	Distance L2	2500
CGH size[a]		94.4	Distance L3	40
Minimum line spacing		18 μm		
Separated distance[b]	(0, 2)	1.3	Parameters of illumination lens	Value (mm)
	(2, 0)	1.2		
	(1, 2)	13	Center thickness	40
	(1,0)	8	Radius	1000
	(−1, 3)	7	Diameter	326
	(3,−1)	5.5	Material	BK7

[a]Main CGH section.
[b]Includes the effect of aperture.

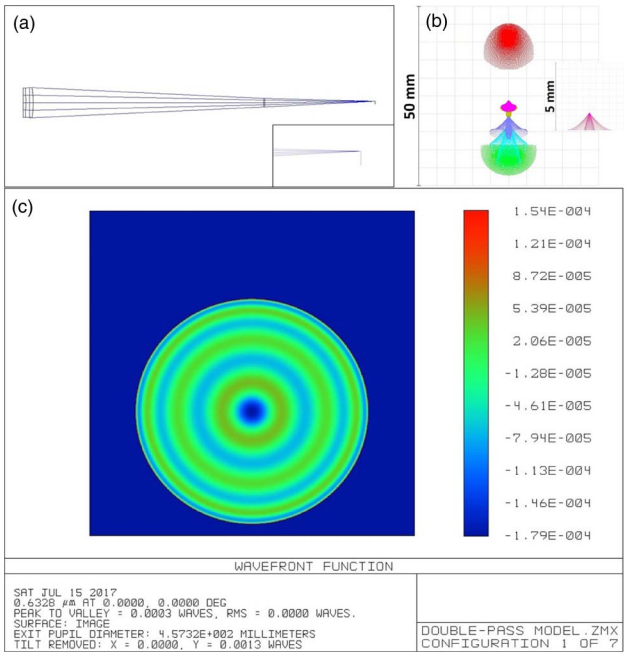

Fig. 6. (a) Design of a configuration used to test the 360.2 mm convex aspheric surface with $R/12.76$. (b) Disturbing diffraction orders are separated on the filter plane, and the typical orders are shown here. Separated distances: 1.3 mm for the order (0,2) (pink), 1.2 mm for the order (2,0) (yellow), 13 mm for the order (1,2) (red), 8 mm for the order (1,0) (green), 7 mm for the order (−1, 3) (blue), and 5.5 mm for the order (3, −1) (cyan). (c) Wavefront function of the configuration. The residual aberration is RMS 0.0000λ, PV 0.0003λ.

(1, 1). Theoretically, the even-order diffraction efficiency of CGH is zero. We here still concentrate on the orders (0, 2) and (2, 0), mainly considering the fabrication errors in the grating depth and the duty cycle, which make the orders (0, 2) and (2, 0) be different from zero [16,17]. The residual aberration of the designed configuration is RMS 0.0000λ, PV 0.0003λ [Fig. 6(c)].

B. Subaperture Stitching Test on the Ultra-Large Convex Aspheric Surface

When the aperture of the convex aspheric surface increases further, which is more than 500 mm, or the $R/\#$ of the surface under test is less than the limitation of this arrangement, we can use this method with the subaperture stitching method together to decrease the area of single measurement, and then, stitch them to get the whole surface figure error. A large convex asphere with $D = 800$ mm ($R/3.75$) is under test, and the parameters are shown in Table 3. This aspherics is an ellipsoid surface, so it cannot be tested in the Hindle sphere method. And also, the diameter of the surface is so large that it needs many subapertures to test the whole area in the conventional

Table 3. Structure Parameters of the Aspheric Surface

Vertex Curvature of Radius/mm	Aspheric Coefficient	Diameter/mm	Material
3000	−0.937	800	SiC

combination of CGH and the subaperture stitching method. In our configuration, it needs just two CGHs to cover the surface. This will improve the efficiency of the test.

The asphere departure and asphere departure slope of this convex surface are shown in Fig. 7. The max value of the asphere departure is more than 40λ, which is quite a large number for aspherics.

We first conduct the subaperture planning for this aspherics, and the subaperture layout is shown in Fig. 8. It needs to design two CGHs in total, one for the central subaperture and the other for the eight outer subapertures, to measure the whole surface. The configurations for the central subaperture and outer subapertures use the same illumination lens. The semi-field angle of the mirror is 3.8141 deg, while the subaperture is 7.5946 deg. The semi-field angle of the effective annular area, which consists of outer subapertures, ranges from 2.15 deg to 8.4019 deg, which overlaps the central subaperture and covers the margin of the aspheric mirror. The diameters of all subapertures are 400 mm, and the central point of the outer subaperture is located at the circle with a radius of 300 mm.

1. Test of Central Subaperture

The parameters of the configuration for the central subaperture ($R/7.5$) are shown in Table 4. The lateral departure of CGH is 20.077 mm, shown in Fig. 9(a). The CGH is fabricated on the 10 mm thick BK7 glass plate and perpendicular to the optical axis. The size of the main CGH section is 168 mm, and the

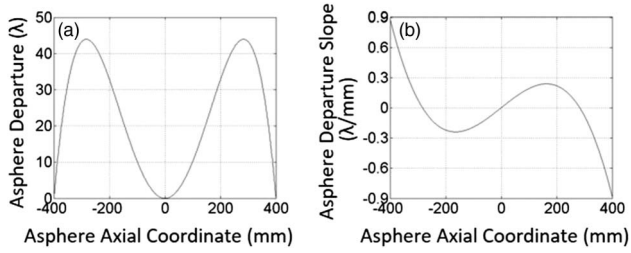

Fig. 7. (a) Asphere departure of the aspheric surface. The max value is more than 40λ. (b) Asphere departure slope of the convex aspheric surface. The max slope is less than 0.9 λ/mm.

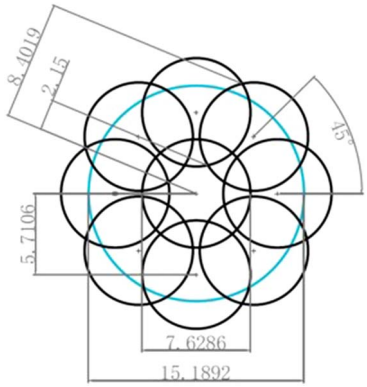

Fig. 8. Subaperture layout of the large convex aspheric surface with $D = 800$ ($R/3.75$). It needs two CGHs and nine apertures in total: one central subaperture and eight outer subapertures.

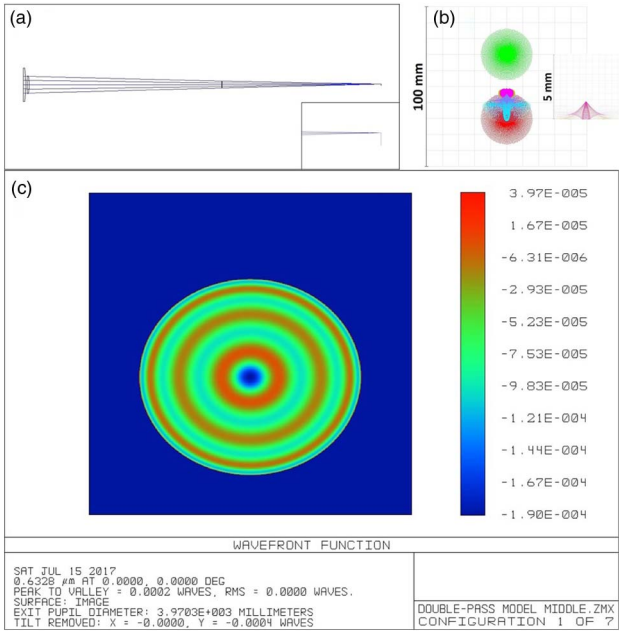

Fig. 9. (a) Design of the configuration used to test the central subaperture of large convex aspherics with $D = 800$ mm ($R/3.75$). (b) Disturbing diffraction orders are separated on the filter plane, and the typical orders are shown here. Separated distances: 1.2 mm for the order (0, 2) (yellow), 1.2 mm for the order (2, 0) (pink), 4 mm for the order (1, 0) (red), 4 mm for the order (1, 2) (green), 5.8 mm for the order (−1, 3) (blue), and 5.0 mm for the order (3, −1) (gray). (c) Wavefront function of the configuration. The residual aberration is RMS 0.0000λ, PV 0.0002λ.

minimum line spacing is 39.7 μm. The diameter of the illumination lens is 420 mm, and the radius of the convex surface of the lens is 1150 mm. All disturbing diffraction orders can be filtered out, shown in Fig. 9(b): 1.2 mm for the order (0, 2) (yellow), 1.2 mm for the order (2, 0) (pink), 4 mm for the order (1, 0) (red), 4 mm for the order (1, 2) (green), 5.8 mm for the order (−1, 3) (blue), and 5.0 mm for the order (3, −1) (gray). The residual aberration of the designed configuration is RMS 0.0000λ, PV 0.0002λ [Fig. 9(c)].

Table 4. Parameters of the System and Designed Optics for the Test of Central Subaperture

Parameters of the CGH		Value (mm)	Parameters of System	Value (mm)
Lateral departure		20.077	Distance L1	3800
CGH thickness		10	Distance L2	4600
CGH size[a]		168	Distance L3	40
Minimum line spacing		39.7 μm		
Separated distance[b]	(0, 2)	1.2	Parameters of illumination lens	Value (mm)
	(2, 0)	1.2		
	(1, 0)	4.0	Center thickness	40
	(1, 2)	4.0	Radius	1150
	(−1, 3)	5.8	Diameter	420
	(3, −1)	5.0	Material	BK7

[a]Main CGH section.
[a]Includes the effect of aperture.

Table 5. Parameters of the System and Designed Optics for the Test of Central Subaperture

Parameters of the CGH		Value (mm)	Parameters of System	Value (mm)
Lateral departure		27.44	Distance L1	4000
CGH thickness		10	Distance L2	4200
CGH size[a]		194	Distance L3	40
Minimum line spacing		36.5 μm		
Separated distance[b]	(0, 2)	1.2	Parameters of illumination lens	Value (mm)
	(2, 0)	1.2		
	(1, 0)	13.5	Center thickness	40
	(1, 2)	14.0	Radius	1150
	(−1, 3)	6.0	Diameter	420
	(3, −1)	5.5	Material	BK7

[a]Main CGH section.
[b]Includes the effect of aperture.

2. Test of Outer Subapertures

The outer annular area has rotational symmetry, so we need to design just one CGH for eight outer subapertures. Taking the subaperture above the central one as an example, the lateral displacement of the outer subaperture is 300 mm, and we tilt the mirror at an angle of 5.712 deg around the z axis and translate 300.0035 mm along the x axis. The illumination lens to be used to test the outer subapertures is the same as the one used for the central subaperture. The parameters of the configuration for the outer subaperture are shown in Table 5. The lateral

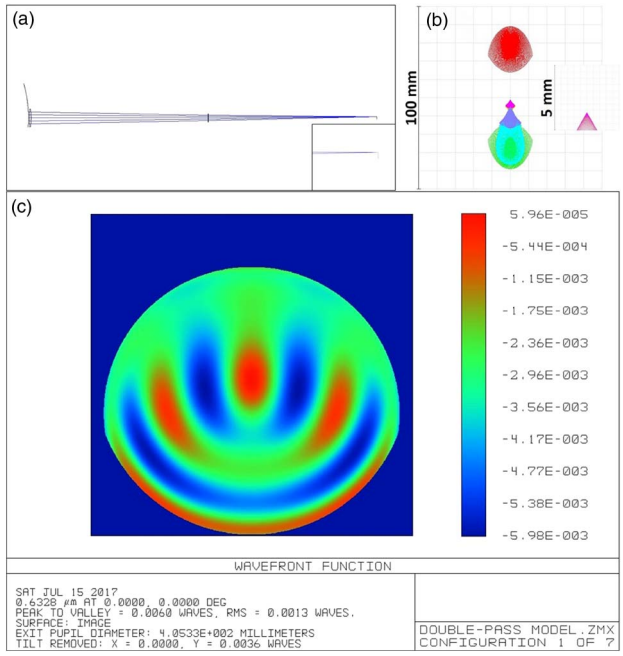

Fig. 10. (a) Design of the configuration used to test the outer subapertures of the aspherics with $D = 800$ mm ($R/3.75$). (b) Spurious diffraction orders are separated on the filter plane, and the typical orders are shown here. Separated distances: 1.2 mm for the order (0, 2) (yellow), 1.2 mm for the order (2, 0) (pink), 13.5 mm for the order (1, 0) (red), 14 mm for the order (1, 2) (green), 6 mm for the order (−1, 3) (blue), and 5.5 mm for the order (3, −1) (gray). (c) Wavefront function of the configuration. The residual aberration is RMS 0.0013λ, PV 0.0060λ.

departure of CGH is 27.44 mm, shown in Fig. 10(a). The CGH is fabricated on the 10 mm thick BK7 glass plate and perpendicular to the optical axis. The size of the main CGH section is 194 mm, and the minimum line spacing is 36.5 μm. All disturbing diffraction orders can be filtered out, shown in Fig. 10(b): 1.2 mm for the order (0, 2) (yellow), 1.2 mm for the order (2, 0) (pink), 13.5 mm for the order (1, 0) (red), 14 mm for the order (1, 2) (green), 6 mm for the order (−1, 3) (blue), and 5.5 mm for the order (3, −1) (gray). The residual aberration of the designed configuration is RMS 0.0013λ, PV 0.0060λ [Fig. 10(c)].

For other outer subapertures, we need just to rotate the convex aspheric surface under test 45 deg every time, and it can be tested just after some fine-tuning. We will get the whole surface figure error after stitching all of the subapertures.

5. SENSITIVITY AND ACCURACY

This setup is not a common path configuration, and thus the perturbations of each optics in this system should be analyzed carefully to determine appropriate tolerances. There are two main types of perturbations: adjusting errors and manufacturing errors. The adjusting errors mainly include the tilt, decentration, and transverse misalignment of CGH and the illumination lens, while manufacturing errors include the refractive index inhomogeneity, surface error, deviation of the radius and center thickness of the illumination lens, and the manufacturing errors of CGH.

We take the design example A, the convex aspheric mirror with $K = -3.662$, $D = 320.8$ mm, and $R = 4093.72$ mm described in Section 3, as the sample of sensitivity analysis. The errors of CGH include a variety of aspects, such as design error, mask fabrication error, substrate error, and so on. These errors of CGH have been analyzed and discussed by many research papers. Summarized from previous studies and the experience of our manufacture, the fabrication errors and design error of CGH can be controlled less than 0.007λ (RMS). Assuming that the errors of this configuration are independent of each other, the test wavefront variation due to manufacture, assembly, and adjustment errors is shown in detail in Table 6.

From the sensitivity analysis, we can get that the deviation of parameters of the illumination lens may have a relatively large effect on the test accuracy. The RSS of wavefront variation is 0.017λ (10.7 nm) [18]. However, it is important to notice that in practice, the CGH and illumination lens are adjusted according to the marks and the interference fringes produced by the fiducial areas and alignment areas of CGH. The process of alignment finishes until acquiring null fringe, so the alignment accuracy can be up to several nanometers. Furthermore, the manufacture errors of the illumination lens can be calibrated in advance, then the CGH can be designed with the actual values of the illumination lens instead of the nominal values. These will further improve the accuracy of this arrangement, which can be better than 6 nm RMS wavefront error (Table 7). Taking the vibration and air disturbance into consideration, the accuracy also can be better than 8 nm (the influence of vibration and air disturbance can be less than 2 nm according to our rich experience). Those aspherics with surface error more than 1 μm could be tested by CMM, while for those large ultra-high precision aspherics ($1/50\lambda \sim 2\lambda$), the method proposed in this paper is measurement physically significant and meaningful.

Table 6. Test Wavefront Variation Due to Manufacture, Assembly, and Adjustment Errors

Parameters		Tolerances	Wavefront Variation (λ)
Distance L1 between focus and CGH		10 μm	0.00015
Distance L2 between CGH and lens		10 μm	0.0027
Distance L3 between lens and asphere		10 μm	0.0015
Tilt of CGH	X	1 μm	0.0004
	Y	1 μm	0.0004
Decentration of CGH	X	1 μm	0.0019
	Y	1 μm	0.0019
Tilt of illumination lens	X	1 μm	0.0073
	Y	1 μm	0.0073
Decentration of illumination lens	X	1 μm	0.003
	Y	1 μm	0.003
Center thickness of illumination lens		10 μm	0.0009
Radius of convex surface of illumination lens		5 μm	0.009
Surface error of illumination lens		$1/100\lambda$	0.004
Refractive index inhomogeneity		$2 * 10^{-6}$	0.003
Synthetical error of CGH			0.007
Substrate error			0.006
Mask fabrication errors			0.003
Residual aberration of design			0.002
Other errors			0.001
RSS			0.017

Table 7. Wavefront Variation with the Careful Alignment and the Calibration of Illumination Lens

Parameters	Tolerances	Wavefront Variation (λ)
Distance L3 between lens and asphere	10 μm	0.0015
Center thickness of illumination lens	10 μm	0.0009
Refractive index inhomogeneity	$2 * 10^{-6}$	0.003
Synthetical error of CGH		0.007
RSS		0.008

6. CONCLUSION

A modified method for testing large convex aspheric surfaces is proposed in this paper. It has some unique advantages compared with existing conventional configurations. This layout utilizes a relatively small specific CGH and the illumination lens to avoid the overly dimensional demand on CGH. One designed illumination lens is universal to a range of convex aspheric surfaces with different parameters, which make this method more convenient. It also can be combined with the subaperture stitching method to cope with ultra-large convex aspheric surfaces. This will improve the measuring efficiency, decrease the accumulation errors, for it enlarges the area of single measurement, and cut down testing cost, for it needs less phase correctors.

Two design examples are given to demonstrate the feasibility and applicability of this method. The residual design error is small enough, and parasitic diffraction orders can be separated

clearly with proper tilt carrier frequency. A series of experiments is operated to testify that this method is applicable to convex aspherics with large $R/\#$ since the dimensional limitation of CGH. Based on the sensitivity analysis, high accuracy can be achieved for this configuration with careful alignment and the calibration of the illumination lens, which can be better than 6 nm RMS.

Actually, this method cannot only test coaxial convex aspherics but also off-axis convex aspheric surfaces and freeform surfaces. Especially for those who do not have SSI equipment and a large transmission sphere, the combination of the illumination lens and CGH proposed in this paper can be a very appropriate alternative. It is economical and highly efficient.

Based on an engineering project, subsequent work is to design and fabricate the CGH and illumination lens to measure the convex aspherics. Further work is required to compare this method with other mature testing methods to confirm the operability of this configuration.

Funding. National Key Research and Development Program (52.5 million RMB).

REFERENCES

1. A. Yabe, "Optimal selection of aspheric surfaces in optical design," Opt. Express **13**, 7233–8242 (2005).
2. J. Li, B. Xuan, and Y. Sun, "Hindle test of SiC convex conic hyperboloid," Proc. SPIE **8417**, 841716 (2012).
3. C. J. Oh, A. E. Lowman, M. Dubin, G. Smith, E. Frater, C. Zhao, and J. H. Burge, "Modern technologies of fabrication and testing of large convex secondary mirrors," Proc. SPIE **9912**, 99120R (2016).
4. M. A. Abdulkadyrov, S. P. Belousov, V. V. Pridnya, A. V. Polyanchikov, and A. P. Semenov, "Optimizing the shaping technology and test methods for convex aspheric surfaces of large optical items," J. Opt. Technol. **80**, 219–225 (2013).
5. J. C. Wyant, "Computerized interferometric surface measurements [Invited]," Appl. Opt. **52**, 1–8 (2013).
6. Y. S. Kim, B. Y. Kim, and Y. W. Lee, "Design of null lenses for testing of elliptical surfaces," Appl. Opt. **40**, 3215–3219 (2001).
7. T. Kim, J. H. Burge, Y. Lee, and S. Kim, "Null test for a highly paraboloidal mirror," Appl. Opt. **43**, 3614–3618 (2004).
8. F. Li, J. Zhao, R. Li, B. Zhang, L. Zheng, and X. Zhang, "Design and fabrication of CGH for aspheric surface testing and its experimental comparison with null lens," Proc. SPIE **7656**, 765643 (2010).
9. Z. Wang, P. Guo, X. Chen, and L. Peng, "Design of null lens system for f/0.5 hyperboloid mirror," Proc. SPIE **9683**, 96831A (2016).
10. P. Murphy, G. DeVries, J. Fleig, G. Forbes, A. Kulawiec, and D. Miladinovic, "Measurement of high-departure aspheric surfaces using subaperture stitching with variable null optics," Proc. SPIE **7426**, 74260P (2009).
11. S. Xue, S. Chen, F. Shi, and J. Lu, "Sub-aperture stitching test of a cylindrical mirror with large aperture," Proc. SPIE **9684**, 96840C (2016).
12. J. H. Burge and D. S. Anderson, "Full-aperture interferometric test of convex secondary mirrors using holographic test plates," Proc. SPIE **2199**, 181–192 (1994).
13. J. H. Burge, D. S. Anderson, T. D. Milster, and C. L. Vernold, "Measurement of a convex secondary mirror using a holographic test plate," Proc. SPIE **2199**, 193–198 (1994).
14. Y. Zhang and Q. Chen, "Testing the large convex aspheric surfaces with aspheric test plate," Proc. SPIE **9280**, 928014 (2014).
15. M. B. Dubin, P. Su, and J. H. Burge, "Fizeau interferometer with spherical reference and CGH correction for measuring large convex aspheres," Proc. SPIE **7426**, 74260S (2009).
16. J. Peng, Z. Chen, X. Zhang, T. Fu, and J. Ren, "Optimal design of tilt carrier frequency computer-generated holograms to measure aspherics," Appl. Opt. **54**, 7433–7441 (2015).
17. J. Peng, J. Ren, X. Zhang, and Z. Chen, "Analytical investigation of the parasitic diffraction orders of tilt carrier frequency computer-generated holograms," Appl. Opt. **54**, 4033–4041 (2015).
18. F. Li, X. Luo, J. Zhao, D. Xue, L. Zheng, and X. Zhang, "Test of off-axis aspheric surfaces with CGH," Opt. Precis. Eng. **19**, 709–716 (2010).